

Wavelength and intensity dependence of multiple forward scattering of electrons at above-threshold ionization in mid-infrared strong laser fields

Chengpu Liu and Karen Z. Hatsagortsyan

Max-Planck-Institut für Kernphysik
Saupfercheckweg 1, D-69117 Heidelberg, Germany

E-mail: k.hatsagortsyan@mpi-k.de

Abstract. The contribution of multiple forward scattering in Coulomb focusing of low-energy photoelectrons at above-threshold ionization in mid-infrared laser fields is investigated. It is shown that the high-order forward scattering can have a nonperturbative effect in Coulomb focusing. The effective number of rescattering events is defined and is shown to depend weakly on laser intensity and wavelength. Nevertheless, the relative contribution of forward scattering in Coulomb focusing and the Coulomb focusing in total decrease with increasing laser intensity and wavelength.

1. Introduction

The Coulomb field of the atomic core can play a significant role in the strong-field photoionization process essentially modifying the dynamics of low-energy electrons. It is responsible, in particular, for the appearance of a rich structure in the momentum distribution of photoelectrons near the ionization threshold [1, 2, 3, 4, 5, 6, 7, 8], for frustrating the tunneling ionization [9] and for the creation of a low-energy structure (LES) in photoelectron spectra in mid-infrared laser fields [10, 11, 12, 13, 14]. The Coulomb field focuses low-energy electrons towards the laser polarization direction which is mostly due to multiple rescattering [15] of ionized electrons by the atomic core at large impact parameters and is termed Coulomb focusing (CF) [16, 17, 18]. For a theoretical description of Coulomb field effects, different modifications of the strong field approximation [19] have been developed [4, 20, 21, 22, 23]. In addition, the classical trajectory Monte Carlo (CTMC) method has been successfully employed, see e.g. [24, 25, 18, 7, 11, 13], for estimation of the effects which are not intrinsically quantum mechanical.

Recently, the strong field physics in mid-infrared laser fields has attracted a lot of attention in connection with the possibility of improving high-order harmonic generation with mid-infrared driver fields [26]. In mid-infrared laser fields, when the Keldysh parameter is small $\gamma = \sqrt{I_p/2U_p} \ll 1$, the electron dynamics after tunneling is mainly classical. This is because the characteristic energies of the process, I_p and U_p , greatly

exceed the photon energy in this regime $\omega \ll I_p \ll U_p$. Here, I_p is the ionization potential, $U_p = E_0^2/4\omega^2$ the ponderomotive energy, E_0 and ω are the laser field amplitude and frequency, respectively (atomic units are used throughout). In this regime, the classical features of the three-step model [15] are conspicuous and not obscured by interference effects. Two recent experiments by Blaga et al. [10] and Quan et al. [11] on the photoionization of atoms and molecules in strong mid-infrared laser fields reveal a characteristic spike-like LES in the energy distribution of electrons emitted along the laser polarization direction. The CF is responsible for the effect [12, 13, 14]. More concretely, the LES arises due to multiple forward scattering (FS) by Coulomb field [13]. The CF is usually predicted to decrease with increase in the laser intensity and wavelength because the average rescattering velocity and the impact parameter increase in such circumstances. As a consequence, one may expect that the contribution of high-order FS should also decrease. In this context, it was surprising that at a large wavelength of the mid-infrared laser field, the multiple FS plays a decisive role for the creation of the LES.

In this paper, we investigate how the contribution of different components of CF depends on laser intensity and wavelength. Our investigation is limited to the classical interaction regime in mid-infrared laser fields. Separate components of CF are identified which scale differently with laser parameters: CF which happens immediately after ionization - initial CF (ICF); CF due to the electron FS on recollision with atomic core, and asymptotic CF (ACF) when the electron momentum is disturbed by the Coulomb field after the laser pulse is switched off. Special attention is devoted to the contribution of the high-order FS events and to the definition of the effective number of FS events. We use the CTMC method with tunneling and the Coulomb field of the atomic core fully taken into account.

2. The method

The 3D CTMC method employed in this paper is developed as follows. (1) An ensemble of electrons is formed corresponding to the tunneled electron wave packet according to the Ammosov-Delone-Krainov (ADK) theory [27]. The electrons are born with the following initial conditions. The electron initial position along the laser polarization direction is derived from the Landau's effective potential theory [28]. The transverse coordinates of the initial position are zero. The initial longitudinal momentum is zero and the transverse one follows the corresponding ADK distribution [29]. (2) The electron wave-packet propagates in the field of a laser pulse and Coulomb potential via the solution of Newton equations. (3) The positions and momenta of electrons when the laser pulse is switched off are used to calculate the asymptotic momenta at the detector [30]. (4) Each trajectory is weighted by the ADK ionization rate and the initial transverse momentum distribution function [29]. (5) The shape of the laser pulse is half-trapezoidal: For the first ten cycles, the field has a constant amplitude and is ramped off within the last three cycles. The electrons are launched within the first half

cycle since there are no multi-cycle interference effects in the classical calculation. The ensemble consists of 10^6 particles and the convergence is checked via double increase of this number. The target atom is neon with ionization potential $I_p = 21.56$ eV which can endure a maximum laser intensity $I_0 \approx 8.66 \times 10^{14}$ W/cm² [31]. The process is in the tunneling regime, e.g., $\gamma \approx 0.2$ at $I_0 = 7.24 \times 10^{14}$ W/cm² and wavelength $\lambda = 2\mu\text{m}$.

We estimate the contributions of the multiple FS, ICF and ACF to the total CF in the following way: (1) For each rescattering event at the moment t_s , the minimal distance from the core r_s , the distance from the core in the transverse plane (with respect to the laser polarization direction) ρ_s and the electron momentum p_s are determined numerically. Then, the transverse momentum change δp_\perp due to the Coulomb potential $V(r)$ at the s -th forward scattering event is estimated as $\delta p_{\perp s} \approx \int \nabla_\perp V(r(t)) dt \sim -(\rho_s/r_s^3)\delta t_s$, where δt_s is the rescattering time duration. When the electron velocity p_s in the FS event is large, $\delta t_s \sim 2r_s/p_s$. In the opposite case, $\delta t_s \sim 2\sqrt{2r_s/|E(t_s)|}$ is determined by the laser field $E(t_s)$ at the s -th rescattering moment t_s . Accordingly,

$$\begin{aligned} \delta p_{\perp s} &= -2\rho_s/(r_s^2 p_s), \quad \text{if } p_s^2 \gg r_s |E(t_s)| \\ \delta p_{\perp s} &= -2^{3/2}\rho_s/\sqrt{r_s^5 |E(t_s)|}, \quad \text{otherwise.} \end{aligned} \quad (1)$$

(2) The transverse momentum change due to ICF is estimated numerically as the deviation of the exact transverse momentum from that neglecting the Coulomb potential, after a half laser period following the ionization moment t_i : $\delta p_\perp^{(I)} = p_\perp(t_i + T/2) - p_\perp^{(NC)}(t_i + T/2)$, where T is the laser period and $p_\perp^{(NC)}$ is the electron transverse momentum neglecting the Coulomb field. The numerical estimate for $\delta p_\perp^{(I)}$ is slightly larger in absolute value than the analytical one [7]:

$$\delta p_\perp^{(I)} \approx -2p_{i\perp} |E(t_i)| / (2I_p)^2, \quad (2)$$

with the initial transverse momentum $p_{i\perp}$. (3) We estimate the ACF contribution via numerical comparison of the asymptotic electron momentum with the one after switching off the laser pulse.

3. The results

The CF is mainly due to multiple small-angle scattering. It is significant only for low energy photoelectrons, and we will examine the dynamics for such electrons in details. The CF is characterized by the transverse momentum change δp_\perp induced by the Coulomb field [13] which depends on the ionization phase $\varphi_i \equiv \omega t_i$. We restrict ourselves to ionization phases and to trajectories which contribute to the low energy part (up to 40 eV) of above-threshold ionization spectrum emitted along the laser polarization direction within an opening angle of $\pm 2.5^\circ$. The electrons, which are emitted out of the laser polarization direction, have experienced large-angle scattering, their CF is interrupted and, consequently, their dynamics is not typical for CF. The laser intensity dependence of the different CF components is shown in Fig. 1 and the wavelength dependence in Fig. 2. For each φ_i , the transverse momentum change is shown for the electron

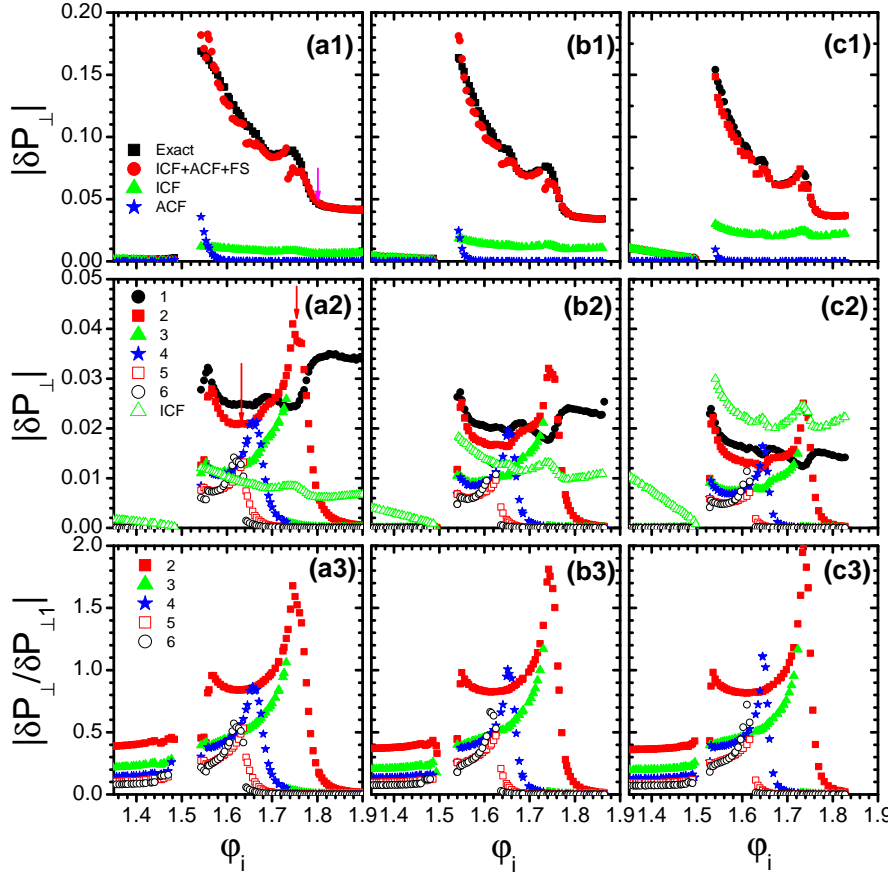


Figure 1. (color online) The transverse momentum change δp_{\perp} versus the ionization phase $\varphi_i = \omega t_i$. The CTMC simulation for a neon atom in a mid-infrared laser field with a wavelength $\lambda = 2\mu\text{m}$ for the following laser intensities: (a1-a3) $I = 1.81 \times 10^{14}$ W/cm², (b1-b3) $I = 3.62 \times 10^{14}$ W/cm² and (c1-c3) $I = 7.24 \times 10^{14}$ W/cm². (a1,b1,c1) The total transverse momentum change (marked as “exact”), the estimation of ICF and ACF as well as of the total transverse momentum change (marked as “ICF+ACF+FS”) as described in Sec.2. (a2,b2,c2) δp_{\perp} due to the s -th order FS events (s is indicated in the inset) and due to ICF. (a3,b3,c3) The ratio of the δp_{\perp} at the s -th order FS events to the first-order one. The ionization phase $\varphi_i^{(1)}$ corresponding to the threshold of the multiple FS is marked by an arrow in (a1). The peak and the plateau of δp_{\perp} for the 2nd FS are marked by arrows in (a2). The maximum of the laser field is at $\varphi_i = \pi/2$.

trajectory which has the maximal probability among the contributing trajectories at this ionization phase. We calculate the total transverse momentum change exactly via the CTMC simulation, see the curves marked as “exact” in Figs. 1 (a1,b1,c1) and 2 (a1,b1,c1). Further in Figs. 1 and 2, we show the results of the estimate of δp_{\perp} due to the s -th FS ($s \leq 6$), ICF and ACF as described in Sec.2. To show the accuracy of our estimations, we sum up all contributions to δp_{\perp} and compare it with the exact result, see the curves marked as “ICF+ACF+FS” in Figs. 1 (a1,b1,c1) and 2 (a1,b1,c1).

From the analysis of Figs. 1 and 2, the following conclusions can be drawn. First of all, Figs. 1 (a1,b1,c1) and 2 (a1,b1,c1) show that the contribution of ACF to the

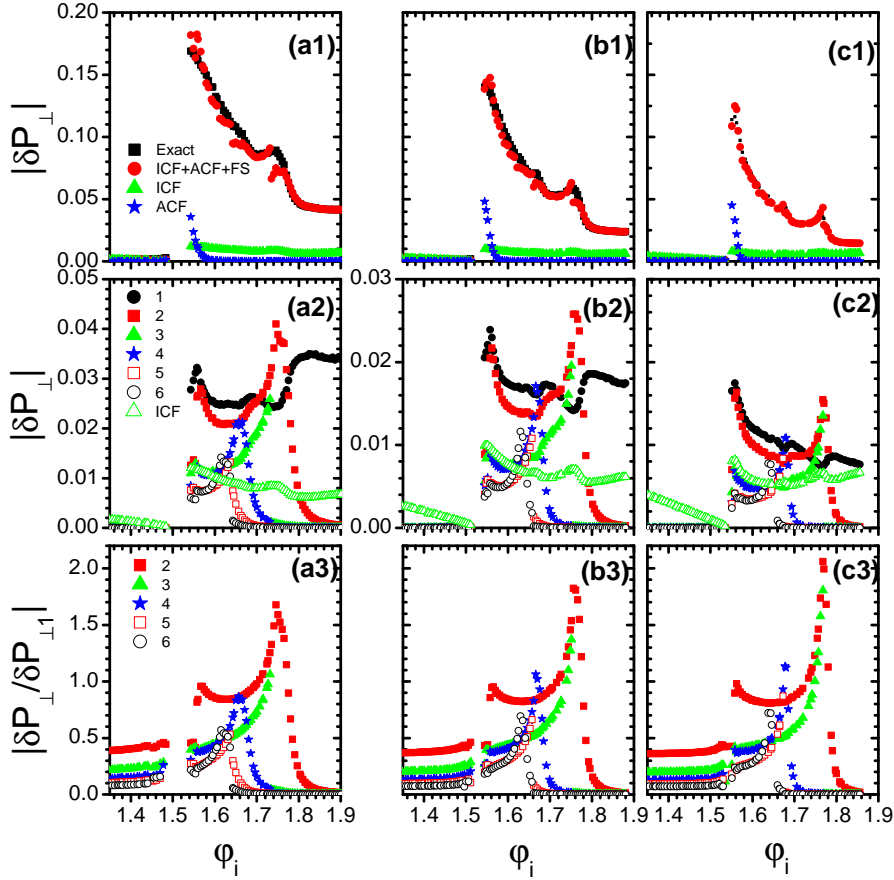


Figure 2. (color online) The transverse momentum change δp_{\perp} versus the ionization phase φ_i . The CTMC simulation for a neon atom in a mid-infrared laser field with an intensity of $I = 1.81 \times 10^{14} \text{ W/cm}^2$ for the following wavelengths: (a1-a3) $\lambda = 2 \mu\text{m}$, (b1-b3) $\lambda = 2.828 \mu\text{m}$ and (c1-c3) $\lambda = 4 \mu\text{m}$. (a1,b1,c1) The total transverse momentum change (marked as “exact”), the estimation of ICF and ACF as well as of the total transverse momentum change (marked as “ICF+ACF+FS”) as described in Sec.2. (a2,b2,c2) δp_{\perp} due to the s -th order FS events (s is indicated in the inset) and due to ICF. (a3,b3,c3) The ratio of the δp_{\perp} at the s -th order FS events to the first-order one.

total δp_{\perp} is generally negligible (the main contribution is at ionization phases near the peak of the laser field within the ionization phase interval of $\delta\varphi_i \approx 0.02$). It decreases with increasing intensity and does not change with wavelength. The contribution of ICF to the total δp_{\perp} increases with increasing intensity and remains almost constant with wavelength which is consistent with the estimate of Eq. (2). The contribution of ICF still constitutes a small fraction of the total δp_{\perp} (less than 10%) for ionization phases $\pi/2 < \varphi_i < \varphi_i^{(1)}$ (the maximum of the laser field is at $\varphi_i = \pi/2$), where multiple scattering takes place but competes with the single scattering contribution at $\varphi_i > \varphi_i^{(1)}$, especially at high intensities and wavelengths (see the estimate below, Eq. (6)). The ionization phase $\varphi_i^{(1)}$ marks the threshold of the multiple FS, see the indication of $\varphi_i^{(1)}$ in Fig. 1 (a1); $\varphi_i^{(1)} \approx 1.8$ at a laser intensity of $1.8 \times 10^{14} \text{ W/cm}^2$ but decreases slightly

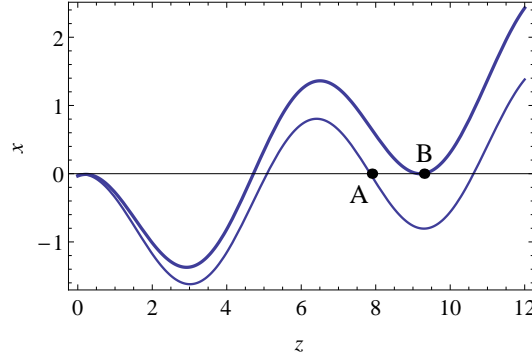


Figure 3. The electron trajectories at $\varphi_i = 1.75$ (thick line) and $\varphi_i = 1.64$ (thin line). The x -coordinate along the laser polarization direction is scaled by E_0/ω^2 and the transverse z -coordinate by $p_{i\perp}/\omega$. The position A corresponds to the plateau and B to the peak of the transverse momentum change at the second forward scattering.

with increasing intensity.

The main CF contribution to the total δp_{\perp} comes from FS which determines the shape of the curve δp_{\perp} versus the ionization phase, shown in Figs. 1 (a1,b1,c1) and 2 (a1,b1,c1). The transverse momentum change $\delta p_{\perp s}$ due to the s -th order FS in the case of different laser intensities and wavelengths are shown in Figs. 1 (a2,b2,c2) and 2 (a2,b2,c2), respectively. $\delta p_{\perp s}$ has a characteristic dependence on the electron ionization phase which is qualitatively the same for each scattering order. The $\delta p_{\perp s}$ increases sharply with decrease in the ionization phase from the threshold value (it is different for different scattering orders), reaches the peak and then decreases slowly down to a flat plateau, the latter having an increasing tail with the further decrease of the ionization phase. Although the contribution of FS decreases on average with increasing order, a higher-order FS can make a larger contribution in some phase intervals than a lower-order one.

Let us estimate the values of the peaks and plateaux of the transverse momentum change due to high-order FS. The peak in the $\delta p_{\perp s}$ for the s -th order FS arises when the electron trajectory touches the z -axis at a recollision (the coordinate center is chosen at the atomic center, x -axis is in the laser polarization direction and z -axis in the transverse direction, see Fig. 3). In this case, $r_s \approx \rho_s$, $E(t_s) \approx E_0$, the electron momentum p_s is nearly zero, see Fig. 4 (a-d), and $\delta p_{\perp s}$ is determined by the second expression of Eq. (1). The ionization phases corresponding to the peak and the plateau of the s -th order FS are indicated in Fig. 4 by $\varphi_{is}^{(p)}$ and $\varphi_{is}^{(pl)}$, respectively. The impact parameter at the peak of the s -th order FS can be estimated as $\rho_s^{\text{peak}} \sim p_{i\perp} \pi (s+1) / \omega$, see Fig. 3. Then, using Eq.(1) we have

$$|\delta p_{\perp s}^{\text{peak}}| \sim \frac{1}{\sqrt{E_0}} \left(\frac{2\omega}{\pi p_{i\perp} (s+1)} \right)^{3/2}. \quad (3)$$

The plateau in the $\delta p_{\perp s}$ corresponds to the FS case when the electron velocity in the FS point is the largest, see Fig. 4 (c). The latter is determined by the amplitude of

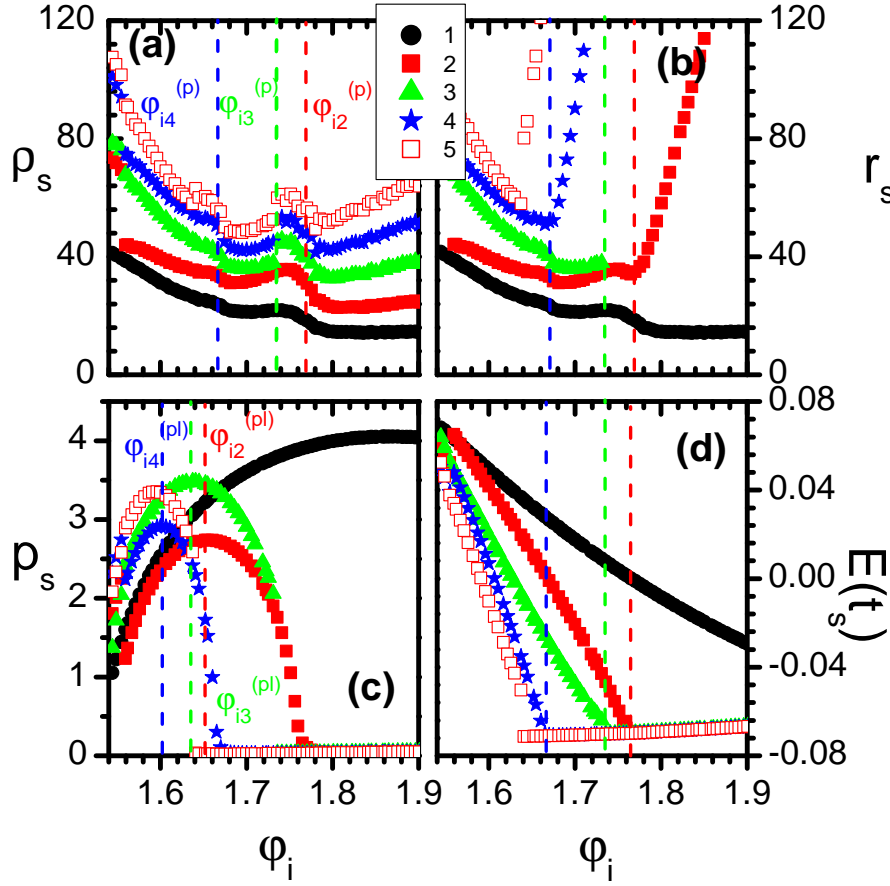


Figure 4. (color online) The parameters of the s -th order FS (s is indicated in the inset): (a) ρ_s the distance from the atomic core in the transverse plane, (b) r_s the distance from the core, (c) p_s the momentum, (d) $E(t_s)$ the field at the scattering moment. $\varphi_{i_s}^{(p)}$ and $\varphi_{i_s}^{(pl)}$ are the ionization phases corresponding to the peak and plateau for the s -th order FS, respectively, which are indicated with dashed lines. The CTMC simulation for a neon atom in a laser field with $I = 1.81 \times 10^{14} \text{ W/cm}^2$ and $\lambda = 2 \mu\text{m}$.

the velocity oscillation in the laser field: $v_s \approx \beta_s E_0 / \omega$, with $\beta_s \approx 0.8$ at even s and $\beta_s \approx 1$ at odd s , according to the numerical results. The impact parameter in this case is estimated as $\rho_s^{\text{plateau}} \sim p_{i\perp} \pi s / \omega$, which yields

$$|\delta p_{\perp s}^{\text{plateau}}| \sim \frac{2\omega^2}{\pi p_{i\perp} E_0 \beta_s s}. \quad (4)$$

The estimates of Eqs. (3) and (4), which are in agreement with the numerical calculations presented in Figs. 1 and 2, show that the peaks for the higher order FS ($(s+1)$ -th order) can exceed the plateaux of the lower-order FS (s -th order). In fact, this ratio is

$$|\delta p_{\perp s+1}^{\text{peak}}| / |\delta p_{\perp s}^{\text{plateau}}| \approx \sqrt{\frac{2E_0}{\pi p_{i\perp} \omega}} \frac{s \beta_s}{(s+2)^{3/2}}, \quad (5)$$

which is between 1.1 and 1.2 for $s = 2 - 6$ at $1.81 \times 10^{14} \text{ W/cm}^2$. Especially, the peaks

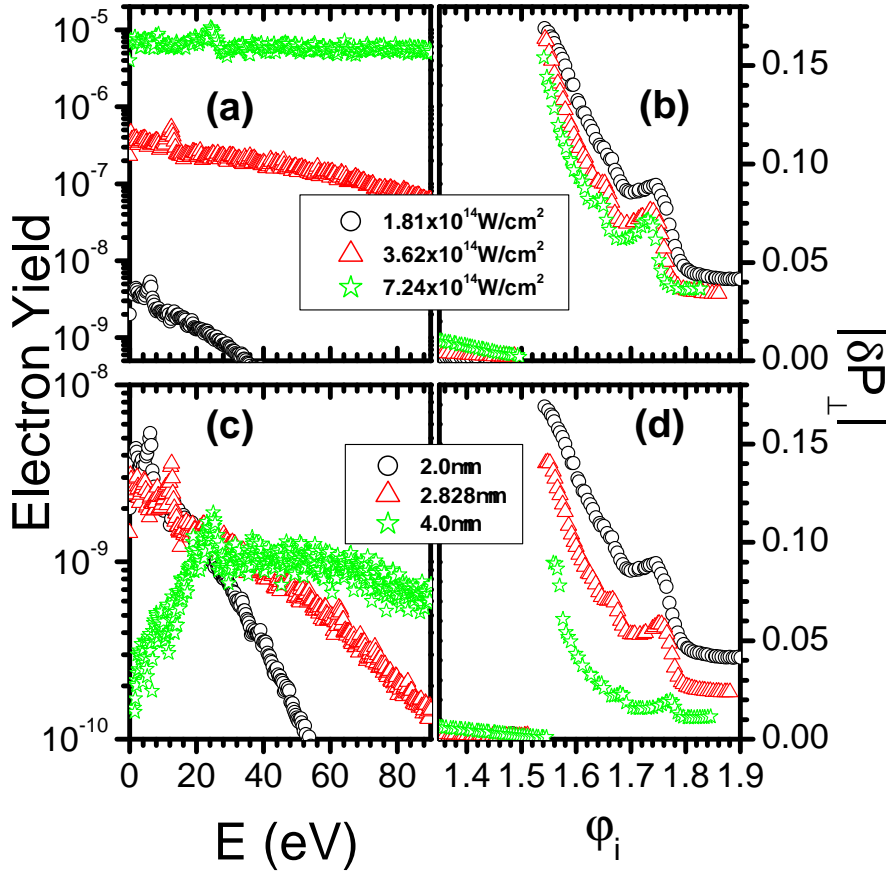


Figure 5. (color online) The CTMC simulation for a neon atom in a mid-infrared laser field: (a,c) Photoelectron spectra. (b,d) The transverse momentum change versus φ_i . (a,b) $\lambda = 2\mu\text{m}$ for different laser intensities indicated in the inset. (c,d) $I = 1.81 \times 10^{14} \text{W/cm}^2$ for different wavelengths indicated in the inset.

of the even order FS (2nd, 4th,...) are larger than the corresponding odd FS plateaux (1st, 3rd,...). The plateaux of the even order (2nd, 4th,...) FS are comparable with that of the corresponding odd FS (1st, 3rd,...). These are because the velocity at even FS events is smaller than that at odd FS. Eq. (5) shows a remarkable feature that the peak-to-plateau ratio increases with increasing intensity and wavelength. In particular, due to a larger contribution of the 6th order FS peak with respect to the plateau of the 5th order FS at intensity $7.24 \times 10^{14} \text{W/cm}^2$, see Fig. 1 (c2), an additional oscillation in the δp_{\perp} dependence on the ionization phase arises, at $\varphi_i \approx 1.64$ in Fig.5 (b), which induces an additional lower energy peak (at about 9 eV) in the energy distribution within the LES, see Fig. 5 (a).

Using Eqs. (2) and (4), we calculate the ratio of ICF to the plateau of the first-order FS:

$$\frac{\delta p_{\perp}^{(I)}}{\delta p_{\perp 1}^{\text{plateau}}} = \pi \left(\frac{p_{i\perp} E_0}{2I_p \omega} \right)^2. \quad (6)$$

The latter confirms the above statement that ICF can compete with the single scattering

contribution to CF at high intensities and wavelengths. For instance, at typical parameters $p_{i\perp} = 0.1$ a.u., $I_p = 0.79$ a.u., $I = 7 \times 10^{14} \text{W/cm}^2$ and $\lambda = 2\mu\text{m}$ the ratio in Eq. (6) amounts to $\delta p_{\perp}^{(I)}/\delta p_{\perp 1}^{\text{plateau}} \approx 0.4$.

The contribution of the FS (as well as the total CF effect) decreases with increasing intensity and wavelength because of the increased scattering velocity and the impact parameter, see Eqs. (3) and (4). For the same reason the curves in the phase space move down with higher intensities and wavelengths in Figs. 5 (b) and 5 (d). However, the ratio of δp_{\perp} of different scattering orders does not significantly vary with variation of laser intensity and wavelength. Thus, the peak of the transverse momentum change due to the s -th FS scaled with that of the first FS can be estimated

$$|\delta p_{\perp s}^{\text{peak}}|/|\delta p_{\perp 1}^{\text{plateau}}| \approx \sqrt{\frac{2E_0}{\pi p_{i\perp} \omega}} \frac{1}{(s+1)^{3/2}}. \quad (7)$$

It shows that the relative role of the s -th FS even increases slowly with increasing laser intensity and wavelength. This can also be seen from Figs. 1 (a3,b3,c3) and 2 (a3,b3,c3). The mentioned feature can be interpreted as a slow variation of the effective number of scattering.

4. The effective number of scattering

The effective number of scattering N_{eff} can be defined employing Eqs. (3) and (4). We define N_{eff} as follows. First of all, we choose a small parameter $\epsilon \ll 1$ to determine the accuracy in which the contributions of the high-order FS to the total δp_{\perp} can be neglected with respect to that of the first FS $\delta p_{\perp 1}$. The effective number of FS N_{eff} is defined to determine the highest order of FS which makes nonnegligible contribution to the total δp_{\perp} . Namely, at a given ϵ ,

$$\begin{aligned} \delta p_{\perp s}^{\text{peak}}/\delta p_{\perp 1}^{\text{plateau}} &> \epsilon, & \text{if } s < N_{eff}, \\ \delta p_{\perp s}^{\text{peak}}/\delta p_{\perp 1}^{\text{plateau}} &< \epsilon, & \text{if } s > N_{eff}. \end{aligned} \quad (8)$$

The latter definition yields the following expression for the effective number of FS

$$N_{eff} \approx \frac{1}{\epsilon^{2/3}} \left(\frac{2 E_0}{\pi \omega p_{i\perp}} \right)^{1/3} - 1. \quad (9)$$

For the intensity range shown in Fig. 1, our criterion gives for N_{eff} a number between 5 and 6 (for the concreteness $\epsilon = 0.1$ is assumed). The number of scattering according to Eq.(9) increases slowly with increase in the laser intensity and wavelength.

Generally, the total CF effect decreases with intensity and wavelength because the main contribution in CF comes from the multiple forward scattering which, in total, decreases as expected, see Fig. 5 (b) and (d), where the curves in the phase space move down, generally, with increasing laser intensity and wavelength. The exception is the tail at $\varphi_i > \varphi_i^{(1)}$ in Fig. 5 (b) which is due to the competition of the first FS with the initial CF as mentioned above. The most important property is that the ratio of the transverse momentum changes due to FS of different orders are almost constant with increasing

laser intensity and wavelength, see Figs. 1 (a3,b3,c3) and 2 (a3,b3,c3). Therefore, the shape of the phase space distribution (dependence of δp_{\perp} on the ionization phase) remains similar, see Fig. 5 (b) and (d). Note that the consecutive slope changes of the phase space distribution are responsible for the creation of LES and are determined by the contributions of the second, third and fourth FS [13].

We point out some features which distinguish the wavelength dependence of CF from the intensity dependence, see Fig. 2. The FS contribution to the total δp_{\perp} decreases more strongly with increasing wavelength as Eqs. (3) and (4) indicate. Due to the latter, the knee of the phase space distribution becomes less prominent at higher wavelengths. The relative contribution of ICF to the total δp_{\perp} with respect to FS increases with increasing wavelength but to a lesser extent than in the case of the intensity dependence. This is because of the $p_{i\perp}$ factor in Eq. (6) which decreases with increase in the wavelengths.

5. Conclusion

At above-threshold ionization in the realm of intensities and wavelengths corresponding to the classical regime $\omega \ll I_p$ and $\gamma \ll 1$, multiple forward scattering of an ionized electron has a nonperturbative contribution to Coulomb focusing. In some regions of ionization phase (photoelectron energy), the contribution of the higher-order forward scattering to the total Coulomb focusing can dominate the lower-order one which creates local peaks in the photoelectron spectra. The effective number of scattering does not depend significantly on laser intensity and wavelength.

Acknowledgments

The fruitful discussions with C. H. Keitel are acknowledged.

References

- [1] Moshhammer R *et al.* 2003 *Phys. Rev. Lett.* **91** 113002
- [2] Rudenko A *et al.* 2004 *J. Phys. B* **37** L407
- [3] Maharajan C M 2006 *J. Phys. B* **39** 1955
- [4] Faisal F and Schlegel G 2005 *J. Phys. B* **38** L223
- [5] Arbo D G *et al.* 2006 *Phys. Rev. Lett.* **96** 143003
- [6] Wickenhauser M *et al.* 2006 *Phys. Rev. A* **74** 041402(R)
- [7] Shvetsov-Shilovski N I *et al.* 2009 *Laser Phys.* **19** 1550
- [8] Burenkov I *et al.* 2010 *Laser Phys. Lett.* **7** 409
- [9] Nubbemeyer T *et al.* 2008 *Phys. Rev. Lett.* **101** 233001
Eichmann U *et al.* 2009 *Nature* **461** 1261
- [10] Blaga C *et al.* 2009 *Nature Phys.* **5** 335
Catoire F *et al.* 2009 *Laser Phys.* **19** 1574
- [11] Quan W *et al.* 2009 *Phys. Rev. Lett.* **103** 093001
- [12] Faisal F 2009 *Nature Phys.* **5** 319
- [13] Liu C and Hatsagortsyan K Z 2010 *Phys. Rev. Lett.* **105** 113003

- [14] Yan Tian-Min , Popruzhenko S V, Vrakking M J, and Bauer D 2010 *Phys. Rev. Lett.* **105** 253002
- [15] Schafer K J *et al.* 1993 *Phys. Rev. Lett.* **70** 1599
Corkum P 1993 *Phys. Rev. Lett.* **71** 1994
- [16] Brabec T, Ivanov M Yu, and Corkum P B 1996 *Phys. Rev. A* **54** R2551
- [17] Yudin G L, and Ivanov M Yu 2001 *Phys. Rev. A* **63** 033404
- [18] Comtois D *et al.* 2005 *J. Phys. B* **38** 1923
- [19] Keldysh L 1964 *Sov. Phys. JETP* **20** 1945
Faisal F 1973 *J. Phys. B* **6** L89
Reiss H 1980 *Phys. Rev. A* **22** 1786
- [20] Duchateau G, *et al.* 2001 *Phys. Rev. A* **63** 053411
- [21] Chen Z *et al.* 2006 *Phys. Rev. A*, **74** 053405
- [22] Yudin G L *et al.* 2007 *J. Phys. B* **40** F93
Yudin G L, Patchkovskii S and Bandrauk A D 2008 *J. Phys. B* **41** 045602
- [23] Popruzhenko S V, Paulus G G, Bauer D 2008 *Phys. Rev. A* **77** 053409
Popruzhenko S V, Bauer D, 2008 *J Mod. Opt.* **55** 2573
- [24] Hu B, Liu J, and Chen S G 1997 *Phys. Lett. A* **236** 533
- [25] Dimitriou K I, *et al.* 2004 *Phys. Rev. A* **70** 061401(R)
- [26] Colosimo P *et al.* 2008 *Nature Phys.* **4** 386
- [27] Perelomov A M, Popov V S and Teren'ev V M 1967 *Zh. Eksp. Teor. Fiz.* **52** 514 [1967 *Sov. Phys. JETP* **25** 336]
Ammosov M V, Delone N B and Krainov V P 1986 *ibid.* **91** 2008 [1986 *ibid.* **64** 1191]
- [28] Landau L D and Lifshitz E M 1977 *Quantum Mechanics* (Pergamon, Oxford) p. 293
- [29] Delone N B and Krainov V P 1991 *J. Opt. Soc. Am. B* **8** 1207
- [30] Landau L D and Lifshitz E M 1993 *Mechanics* (Pergamon, Oxford) p. 170
- [31] Bethe H and Salpeter E 1977 *Quantum Mechanics of Atoms with One and Two Electrons* (Berlin: Springer)